

Dynamics of Intermittent Delayed Emission in Single CdSe/CdS Quantum Dots

Stijn O. M. Hinterding, Sander J. W. Vonk, Elleke J. van Harten, and Freddy T. Rabouw*

Cite This: *J. Phys. Chem. Lett.* 2020, 11, 4755–4761

Read Online

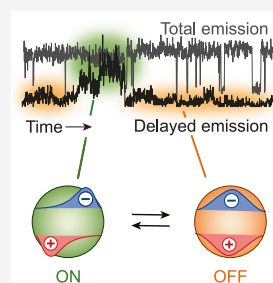
ACCESS |

Metrics & More

Article Recommendations

Supporting Information

ABSTRACT: Bright and fast fluorescence makes semiconductor nanocrystals, or quantum dots (QDs), appealing for applications ranging from biomedical research to display screens. However, a few percent of their fluorescence intensity is surprisingly slow. Research into this “delayed emission” has been scarce, despite undesired consequences for some applications and potential opportunities for others. Here, we characterize the dynamics of delayed emission exhibited by individual CdSe/CdS core/shell QDs and correlate these with changes in the emission spectrum. The delayed-emission intensity from a single QD fluctuates strongly during an experiment of several minutes and is thus not always “on”, implying that control over delayed emission may be possible. Periods of bright delayed emission correlate with red-shifted emission spectra. This behavior is consistent with exciton polarization by fluctuating electric fields due to diffusing surface charges, which have been known to cause spectral diffusion in QDs. Our findings thus provide a stepping stone for future efforts to control delayed emission.



Research and development for over 25 years¹ has resulted in high-quality semiconductor nanocrystals (or quantum dots, QDs) of various material compositions that produce bright fluorescence useful in display screens, lighting, bioimaging, quantum optics, and other applications.² Nevertheless, some of their key fundamental properties remain poorly understood. For example, while the excited state of a QD usually lives no longer than a few tens of nanoseconds before it decays by emitting a photon, sometimes emission takes orders of magnitude longer.^{3–15} This slow emission—or “delayed emission”—is responsible for on the order of 10% of the fluorescence from various types of QDs, including CdSe/CdS/CdZnS/ZnS core/multishells,¹⁰ Cu-doped CdSe,¹³ CuInS₂,¹³ and lead-halide perovskites.¹⁴ It is typically ascribed to trapping and detrapping of excited charge carriers, which renders the excited state of the QD temporarily nonemissive. The prolonged excited-state lifetimes can be beneficial for the use of QDs in photocatalysis and photovoltaics. On the other hand, the occurrence of (temporarily) nonemissive excited states may have negative implications for the use of QDs as laser gain medium¹⁶ or as Förster resonance energy transfer (FRET) donors.⁷ Furthermore, delayed-emission trapping has been tentatively linked to fluorescence blinking of single QDs^{3–6,8–11,13,15} and may lower the threshold for fluorescence saturation.^{6,17}

Most of what we know about delayed emission has until now come from ensemble-scale experiments. Generally, the decay of delayed emission following pulsed excitation is characterized by a long, power-law-like slope,^{3,10–13,15} indicating broadly distributed rates of charge-carrier detrapping. (De)trapping of charge carriers likely happens through tunneling, as the rates are temperature-independent.^{11,13,18,19} The trapping process is

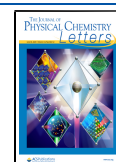
thought to occur from the lowest-energy exciton state.^{3–6,8–15} Based on the spectrum of delayed emission on the ensemble scale, the lowest-energy exciton is likely restored upon charge-carrier detrapping, followed by radiative recombination.^{10,12–14} However, much is still unknown regarding delayed emission. For example, ensemble-scale experiments do not provide information about variations between QDs or dynamic fluctuations that likely underly the distributed dynamics of delayed emission. Moreover, ensemble-averaging masks possible correlations between the fluorescence intensity, dynamics, and spectrum, which could otherwise establish the mechanisms of trapping/detrapping and the proposed link between delayed emission and blinking.

Here, we elucidate the mechanisms underlying delayed emission in individual CdSe/CdS core/shell QDs, using a combination of single-QD spectroscopy and time-correlated single-photon counting (TCSPC). Low-dark-count detectors allow us to measure the photoluminescence (PL) decay dynamics of single QDs up to 1 μ s after excitation with negligible (<20 photons/s) background. All single QDs measured have prompt PL lifetimes of approximately 30–50 ns but also show delayed emission on time scales until 1 μ s. Surprisingly, the intensity of delayed emission shows strong temporal fluctuations, seemingly uncorrelated to fluctuations of

Received: April 24, 2020

Accepted: May 27, 2020

Published: May 27, 2020



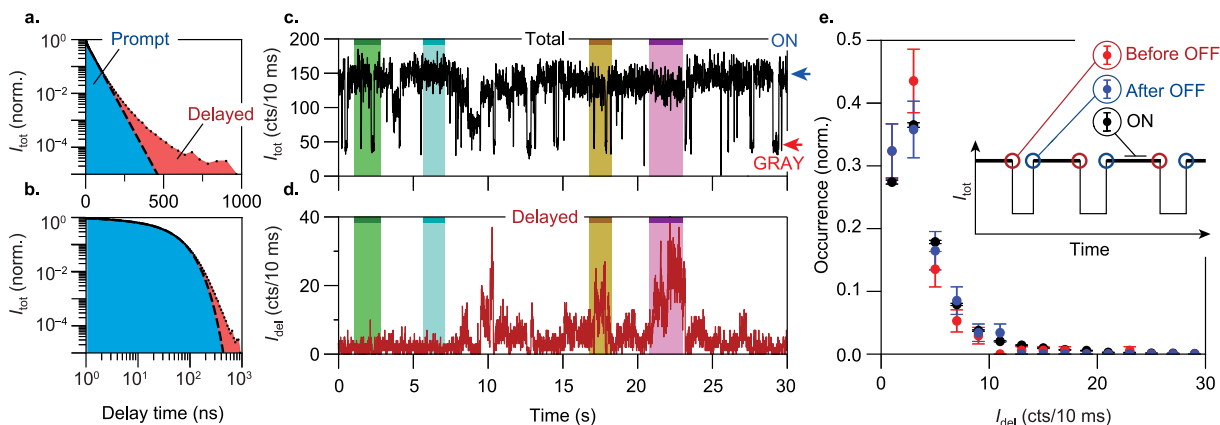


Figure 1. (a,b) Normalized PL decay curves of a single CdSe/CdS core/shell QD, displayed on (a) semilogarithmic and (b) log–log scale. The dashed lines are a biexponential fit to the data up to a delay time of 100 ns. Prompt and delayed emission are indicated with blue and red shading, respectively. (c) Total photoluminescence (PL) intensity (I_{tot}) trace of an individual quantum dot (QD), constructed with a 10 ms bin size. I_{tot} switches between a state of high and a state of lower intensity labeled “ON” (blue arrow) and “GRAY” (red arrow). The background intensity is 0.2 cts/10 ms. (d) Delayed-PL intensity (I_{del} , defined as the number of photons detected ≥ 200 ns after a laser pulse) trace of the same QD, binned at 10 ms. I_{del} fluctuates between low (3 cts/10 ms) and high (~ 25 cts/10 ms) values. (e) Distributions of I_{del} corresponding to (red) bins directly preceding an ON \rightarrow GRAY switch (i.e., selecting all bins i for which $I_{\text{tot},i+1} - I_{\text{tot},i} \leq -70$ cts/10 ms), (blue) bins directly following a GRAY \rightarrow ON switch (i.e., $I_{\text{tot},i} - I_{\text{tot},i-1} \geq 70$ cts/10 ms), and (black) all 10 ms time bins during which the QD is ON ($I_{\text{tot},i} \geq 100$ cts/10 ms).

the total emission intensity (i.e., blinking). We find that the QD emission spectrum is red-shifted and broadened during time periods of high delayed-emission intensity. These spectral changes are reminiscent of the response of a QD to an external electric field, due to the quantum-confined Stark effect (QCSE).^{20–30} However, the QCSE alone cannot explain the very slow dynamics of delayed emission. We propose that, additionally, polarization of the exciton by the spontaneously fluctuating electric field facilitates temporary trapping of charge carriers, as was previously observed for applied external electric fields.²³ Our results establish delayed emission as yet another property of QDs with pronounced temporal fluctuations, besides the total fluorescence intensity (i.e., blinking) and their spectrum (i.e., spectral diffusion).

We synthesized CdSe/CdS core/shell quantum dots (QDs) with an ensemble emission peak at 628 nm (Figure S1) and a diameter of 8.4 ± 1.7 nm (mean \pm standard deviation; Figure S2) following a procedure based on the work of Chen et al.³¹ The PL decay dynamics of a typical single CdSe/CdS QD from our batch (Figure 1a,b) are similar to those of the ensemble (Figure S3). The decay is approximately exponential on the first 50 ns due to “prompt” radiative recombination of the exciton, i.e., directly following photoexcitation. The slower nonexponential tail is denoted “delayed emission” and is typically ascribed to temporary trapping of one (or both) charge carriers from the band-edge state, followed by detrapping and subsequent radiative recombination of the exciton.^{3–5,8–15} All 10 QDs studied in detail showed nonexponential delayed emission, consistent with previous studies,³ although the relative intensity of delayed compared to prompt emission varied between QDs (see Extended Data, Figures E1–10). Distributed dynamics are thus not only an ensemble-averaged characteristic of delayed emission but also an intrinsic property of individual QDs.

Under continued photoexcitation, the CdSe/CdS QD discussed here blinks between a high-intensity state producing 137 photon counts/10 ms and a lower-intensity state with 42 photon counts/10 ms (Figure 1c). The characteristics of these states (see Extended Data, Figures E1–10) are consistent with

an “ON” state, in which the QD exhibits a PL quantum yield (QY) of unity,³² and a “GRAY” state, in which the QD is momentarily charged, leading to an increased radiative decay rate but a reduced PLQY because of competition with nonradiative Auger decay processes.^{33,34}

In Figure 1d, we show the delayed-emission intensity, I_{del} , over the same measurement period of 30 s as shown in Figure 1c. For this analysis, we classify a photon as “delayed” when it is detected more than 200 ns after the laser pulse. As the PL lifetime of the ON states of our QDs is 30–50 ns, a threshold of 200 ns effectively discards $>99\%$ of the exponential prompt emission while accepting enough delayed photons to allow further analysis. We observe, surprisingly, that the delayed-emission intensity fluctuates strongly, between a low value of ~ 3 counts/10 ms (due to background fluorescence and unrejected prompt emission; Figure S4) to high values of >40 counts/10 ms.

At first glance, it is difficult to identify correlations between the fluctuations in I_{del} and fluctuations in I_{tot} : during ON periods, the QD can exhibit either low or high I_{del} (cyan and purple regions in Figure 1c,d, respectively). Similarly, periods in which the QD is blinking between the ON and GRAY states can exhibit either low or high I_{del} (green and yellow regions in Figure 1c,d, respectively). More quantitative statistical analysis (Figures 1e and S5) does not reveal correlations between I_{del} and I_{tot} either, despite recent proposals for a relationship between delayed emission and blinking.^{3–6,8–11,13,15} We have to stress, however, the gap in time scales between our measurements of delayed emission (between 200–1000 ns after laser excitation) and our ability to resolve blinking (10 ms). We might in fact miss the rarest and slowest delayed-emission events that are the most relevant for blinking. Only when a charge carrier is trapped for $\gg 1$ μs would this effectively charge the QD and thereby lead to an ON \rightarrow GRAY switch observable in the blinking trace of Figure 1c. Ensemble-scale experiments have provided evidence for such very slow detrapping processes.^{10,11,13,15}

Ensemble-scale time-resolved emission spectroscopy (TRES) on our CdSe/CdS QDs dispersed in toluene yields

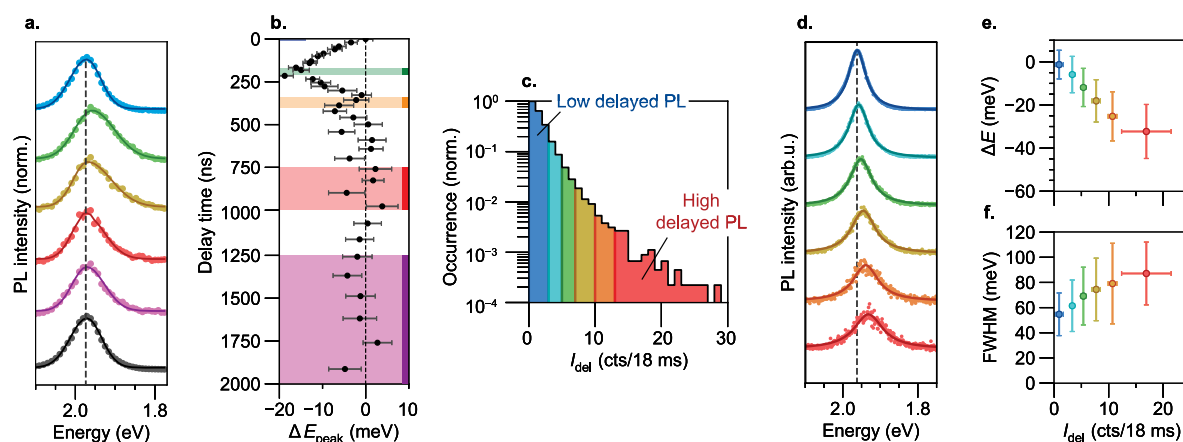


Figure 2. (a) Time-resolved PL spectra of an ensemble of CdSe/CdS QDs dispersed in toluene, obtained by integrating the PL spectrum over delay times of 0–10 ns (blue), 170–210 ns (green), 340–400 ns (yellow), 750–1000 ns (red), 1250–2000 ns (purple), and 0–2000 ns (black). (b) PL peak positions, obtained by fitting spectra with a two-sided Gaussian (see Supporting Information, Section S2 for details). The dashed line is the peak position of the early time spectrum (0–10 ns), which is set to $\Delta E_{\text{peak}} = 0$. Error bars correspond to ± 1 standard error of the fit. (c) Distribution of delayed-emission intensity during simultaneous TCSPC and spectral measurements on the same single QD discussed in Figure 1. For this analysis, we selected only periods during which the QD was ON (i.e., total intensity $I_{\text{tot}} > 75$ cts/18 ms on the single-photon detector). (d) Single-QD PL spectra as a function of I_{del} , obtained by selecting periods of a 296 s experiment during which the QD exhibited delayed-emission intensity (colored regions indicated in panel (c)) of $I_{\text{del}} < 3$ cts/18 ms (blue), $3 \text{ cts/18 ms} \leq I_{\text{del}} < 5$ cts/18 ms (cyan), $5 \text{ cts/18 ms} \leq I_{\text{del}} < 7$ cts/18 ms (green), $7 \text{ cts/18 ms} \leq I_{\text{del}} < 10$ cts/18 ms (yellow), $10 \text{ cts/18 ms} \leq I_{\text{del}} < 13$ cts/18 ms (orange), and $13 \text{ cts/18 ms} \leq I_{\text{del}}$ (red). (e) PL peak position and (f) full-width-at-half-maximum as a function of our selection of I_{del} , displayed here as the mean \pm standard deviation of Lorentzian fits to the selected 18-ms-integrated spectral frames.

results consistent with previous studies:^{10,12–14} the spectrum emitted over the first 10 ns after photoexcitation (blue in Figure 2a) is nearly identical to the delayed-emission spectrum recorded from 1250 to 2000 ns (purple in Figure 2a). This confirms that delayed emission of our QDs involves recombination of free, rather than trapped charge carriers. In contrast, emission involving trapped charges would yield a broad spectrum red-shifted from the lowest-energy exciton recombination, due to strong electron–phonon coupling.^{35–37} On intermediate time scales, between 50 and 400 ns, the spectrum is red-shifted and broadened (Figure 2a,b). This behavior, matching previous TRES measurements on Cd-based QDs,^{10,38} is attributed in the literature to polydispersity in the QD size and corresponding variations in the prompt radiative decay rate.³⁹ As we will show below, spectral diffusion likely contributes to this red-shift as well.

To correlate the spectral properties and delayed-emission dynamics of single QDs, we performed simultaneous time-correlated single-photon counting and spectroscopy by splitting the QD emission (Supporting Information, Section S2). Synchronizing the measurements provides us with the delayed-emission intensity I_{del} of the QD (Figure 2c) during the integration time of each spectral frame. Figure 2d shows the PL spectra for increasing I_{del} . Note, however, that, as the integration time for each spectral frame was 18 ms, these PL spectra always contain contributions from both prompt and delayed emission.

The single-QD PL spectrum contains a single peak for all delayed-emission intensities I_{del} (Figure 2d), resembling a Lorentzian. This indicates that delayed emission is due to recombination of delocalized, rather than trapped, charge carriers. If the delayed emission we study here was due to emission from (surface) trap states, we would expect the appearance of a second, red-shifted peak in the PL spectrum, as commonly observed for trap emission on the ensemble scale.^{35,36} Nevertheless, the PL spectrum for high I_{del} is

different from that for low I_{del} . It red-shifts up to 30 meV with increasing delayed-emission intensity (Figure 2e) and broadens (Figure 2f). As all spectra show a single emission peak, this red-shift corresponds to a spectral shift of both prompt and delayed emission.

The comparison between the time-resolved PL spectra of the QD ensemble (Figure 2a,b) and the single-QD spectra for selected I_{del} (Figure 2d–f) is not straightforward. Even during moments of the highest I_{del} ($I_{\text{del}} > 13$ cts/18 ms, red in Figure 2c), 83% of the emission is emitted at delay times < 200 ns, and only 17% of the emission is emitted at delay times of 200–1000 ns. In our correlated experiments of PL spectra and dynamics, it is impossible to select the slowest delayed emission (> 500 ns) exclusively. This explains why our single-QD analysis reproduces the initial red-shift and broadening of the delayed emission observed in the ensemble-scale TRES data (blue and green spectra in Figure 2a), but it is difficult to observe the blue-shift on time scales > 250 ns (yellow, red, and purple spectra in Figure 2a). Of the 10 QDs studied, only one shows this blue-shift for the highest I_{del} (see QD 5 in the Extended Data, Figures E5 and E15). Regardless, our single-QD experiments prove that the initial red-shift is not exclusively due to sample polydispersity but occurs on the scale of individual QDs. Future experiments yielding simultaneous information on the color and delay time of each individual photon may be necessary to study the single-QD spectrum of the slowest delayed emission (> 500 ns) in more detail.⁴⁰

The spectral red-shift and broadening (see Figure 2) point to an influence of the quantum-confined Stark effect (QCSE)^{25,41} on delayed emission. The QCSE is the response of a nanoconfined semiconductor to an external electric field. For example, with the application of electric fields on the order of 10^7 V m^{-1} ,^{21,23–28} the emission of QDs and nanorods red-shifts and broadens. The QCSE also underlies spectral diffusion, the spontaneous fluctuations in the PL spectrum

demonstrated in various types of individual QDs at cryogenic temperatures as well as room temperature.^{22,25,29,30,32–44} These are due to spontaneously fluctuating electric fields experienced by charge carriers in the QD due to, for example, surface atoms or capping ligands moving around over the QD surface.

To elucidate the possible influence of electric fields on delayed emission in our individual QDs, we analyze the PL decay dynamics in more detail. We scaled the PL decay curves of our QD for increasing I_{del} (Figure 3a,b) to the number of 18

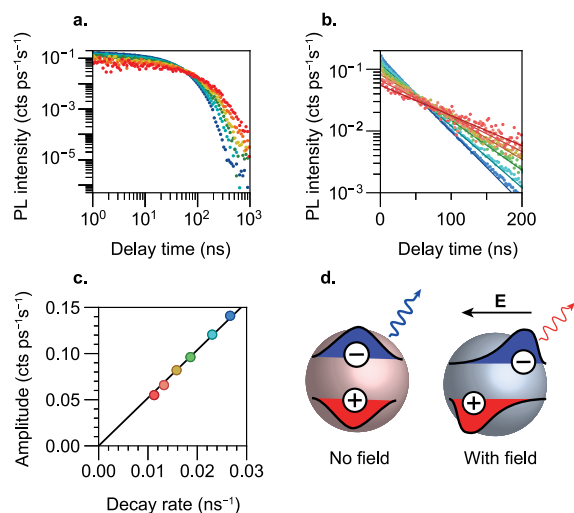


Figure 3. (a) Background-subtracted single-QD PL decay curves from selected periods with increasing delayed-emission intensity I_{del} , corresponding to the six delayed-emission categories indicated in Figure 2c. We select only periods in which the QD is ON (total emission is >75 cts/18 ms). (b) Zoom-in of the PL decay curves of panel (a) on a semilogarithmic scale. Solid lines are monoexponential fits. (c) Amplitude and decay rates obtained from fits of monoexponential decay to the experimental decay curves depicted in (a,b). Colors indicate the delayed-emission category (see Figure 2c). The solid line is a linear fit to the data points. (d) Schematic depiction of the QCSE: an external electric field perturbs the electron and hole wave functions, thereby reducing the electron–hole wave function overlap and decreasing the radiative decay rate k_{rad} .

ms time periods that were selected to generate the curve. The amplitude of the decay curve, i.e., the intensity at delay time $t = 0$, is then proportional to the radiative decay rate of the QD (Supporting Information, Section S3). With increasing I_{del} (from blue to red in Figure 3a,b), the PL decay becomes slower, and the amplitude of the decay curve decreases. Figure 3c shows a linear relation between the early time PL decay rate and the amplitude of the decay curve. This can be qualitatively explained in terms of the QCSE, wherein a fluctuating electric field polarizes the exciton wave function (Figure 3d). Exciton polarization reduces the electron–hole overlap and thereby the radiative recombination rate k_{rad} , to which the amplitude of the decay curve is proportional (Supporting Information, Section S3).

Although the behavior of our single QD is qualitatively consistent with the QCSE, the fluctuations of k_{rad} by a factor 2.4 (Figure 3c) are stronger than have ever been reported. Previous experiments achieved spectral shifts of up to several tens of meV in colloidal QDs and nanorods,^{24,26–28} induced by electric fields of up to 50 MV m⁻¹ applied using external electrodes. The spectral fluctuations of our QD (up to ~35

meV; Figure 2e) are thus consistent with spontaneously fluctuating electric fields with strengths of up to a few tens of MV m⁻¹, which could originate from a few elementary charges diffusing around on the QD surface (see Supporting Information, Section S4 for further discussion of this). However, such fields were previously reported to increase the PL lifetime of individual CdSe/CdS QDs by no more than 5%,²⁴ while the PL lifetime of individual CdSe/ZnS QDs became shorter by ~10% or longer by ~10%, depending on the particular QD.²⁶ These weak lifetime changes are at odds with the strong fluctuations of up to a factor of 2.4 that we observe. The slowest photon emission events in our experiments (e.g., at $t = 500–1000$ ns in Figure 3a) are even more difficult to reconcile with the expected limited effect of the QCSE on the fluorescence lifetime.

To better understand the expected effect of the QCSE on the PL lifetime, we performed simple quantum-mechanical effective-mass calculations (Figure 4). We approximated our

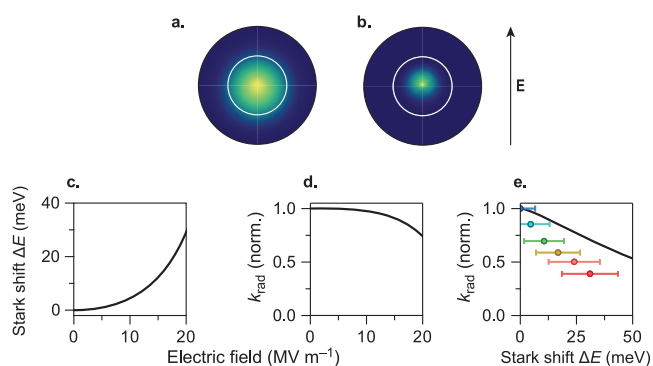


Figure 4. (a,b) Calculated (a) electron and (b) hole charge densities in a CdSe/CdS core/shell QD experiencing a homogeneous electric field in the vertical direction (see arrow) with a strength of 14 MV m⁻¹. See Supporting Information, Section S4 for details of the model. (c) Calculated Stark shift ΔE as a function of electric-field strength. (d) Calculated normalized radiative decay rate, k_{rad} , as a function of electric-field strength. (e) Calculated relation between k_{rad} and ΔE for our QD geometry due to the quantum-confined Stark effect (QCSE, solid line), and experimental single-QD data (colored symbols). Symbol colors refer to the delayed-emission category (see Figure 2c); error bars correspond to ± 1 standard deviation in the fitted Stark shifts.

QDs as spherical particles with a core of 2 nm radius and a shell of 2 nm thickness and calculated the spectral shift and radiative decay rate with increasing homogeneous electric field. The electric field polarizes the exciton wave function (Figure 4a,b), decreases the exciton energy (Figure 4c), and reduces the electron–hole overlap integral and thereby the radiative decay rate (Figure 4d).²⁸ We calculate that a homogeneous field of approximately 20 MV m⁻¹ induces a Stark shift of approximately 35 meV, which is close to the maximum peak shift we and others^{24,26–28} observed experimentally (see Figure 2e). The corresponding PL decay rate, however, is only slower by 25% compared to the zero-field situation. These calculations confirm that the QCSE alone cannot explain the strong fluctuations in lifetime observed experimentally (Figure 4e). Note that in the experiment, the QD may never experience exactly zero electric field, but this does not affect the expected correlation between exciton energy and radiative lifetime based on the QCSE model.

To reconcile the apparent link between the QCSE and delayed emission with the quantitative mismatch between the emission time scales, we propose a mechanistic link between charge-carrier trapping/detrapping and the QCSE. The spontaneously fluctuating electric fields, which induce the QCSE,^{22,25,29,30} may—if sufficiently strong—also promote temporary trapping of charge carriers. Indeed, several delayed-emission characteristics on the ensemble and single-QD levels clearly point to charge-carrier trapping/detrapping. For example, the single-QD PL decay curves at high I_{del} contain lifetime components that are an order of magnitude slower than the prompt lifetime of 40.7 ns (see delay times of 500–1000 ns in Figure 3a), which cannot be understood in terms of the QCSE alone. Moreover, the ensemble-scale emission spectrum at delay times of >400 ns is nearly identical to prompt emission, indicating emission from a nonpolarized exciton.

Our interpretation is supported by previous experiments, which demonstrated that external electric fields can not only induce the QCSE^{24,26–28} but also influence charge-carrier trapping.²³ In fact, a transition has been shown for individual CdSe/ZnS nanorods where weak applied electric fields (<20 MV m⁻¹) result in the QCSE while stronger fields (>20 MV m⁻¹) cause charge-carrier trapping.²⁷ We propose that spontaneous electric-field fluctuations due to a moving surface charge could have similar effects. Weak fluctuating fields result in red-shifted and broadened PL and a reduced radiative recombination rate due to the QCSE. Stronger fluctuating fields result in temporary charge-carrier trapping,²³ giving rise to the red-shifted and unusually slow emission on 100–400 ns time scales. The slowest delayed emission (>400 ns), which is not red-shifted, can be explained as follows: the strongest fluctuating fields induce charge-carrier trapping but may also prevent detrapping (as observed in ref 23 for externally applied electric fields). Hence, charge carriers cannot detrapp until after the field disappears spontaneously. This could lead to the slowest delayed-emission events that have the same spectrum as prompt emission. Indeed, correlation analysis on delayed photons (Figure S6) demonstrates fluctuations in delayed-emission intensity, hence, electric-field fluctuations, on micro-second time scales. These electric-field fluctuations would be responsible for keeping charges trapped for prolonged times of 400 ns and longer.

The delayed-emission characteristics of individual CdSe/CdS QDs and QD ensembles thus provide evidence for a mechanistic link between delayed emission and spectral fluctuations due to the QCSE. Although we studied CdSe/CdS QDs here, exciton wave functions are polarizable by surface charges in other types of QDs as well. This mechanism could thus contribute to the delayed emission observed in many types of QDs, including CuInS₂ and perovskites.^{11,14} Our findings suggest strategies to control or even eliminate the occurrence of delayed emission from colloidal QDs.^{10,13,14} A high-bandgap shell around the emissive QD core would increase the separation from diffusing surface charges and reduce their effect on the exciton. However, charge-carrier delocalization—as in our CdSe/CdS QDs with a quasi-type-I band alignment—counteracts this beneficial effect, because it increases the exciton polarizability and hence the response to external fields. Recently, CdSe/Cd_xZn_{1-x}Se core/shell QDs have been reported, with a type-I band alignment that confines both charge carriers to the core and prevents increased exciton polarizability.⁴⁵ Indeed, these QDs showed reduced spectral

diffusion due to the QCSE. Future research will have to establish whether such new core/shell QD designs can suppress delayed emission. This might, for example, be important to increase the saturation threshold of QDs,¹⁷ making them better suited for high-power and laser applications.

■ ASSOCIATED CONTENT

Supporting Information

The Supporting Information is available free of charge at <https://pubs.acs.org/doi/10.1021/acs.jpcllett.0c01250>.

Experimental methods, further details related to the data processing and analysis, derivation of the relevant rate equations, details on the quantum-mechanical calculations, correlation analysis of delayed photons, determination of the background intensity and the excitation regime, ensemble-scale characterization of the sample (PDF)

Extended Data, containing an overview of results of single-QD measurements on all 10 QDs studied (PDF)

■ AUTHOR INFORMATION

Corresponding Author

Freddy T. Rabouw – *Soft Condensed Matter and Inorganic Chemistry and Catalysis, Utrecht University, 3584CC Utrecht, The Netherlands*; orcid.org/0000-0002-4775-0859; Email: ft.rabouw@uu.nl

Authors

Stijn O. M. Hinterding – *Soft Condensed Matter and Inorganic Chemistry and Catalysis, Utrecht University, 3584CC Utrecht, The Netherlands*; orcid.org/0000-0002-3940-1253

Sander J. W. Vonk – *Soft Condensed Matter and Inorganic Chemistry and Catalysis, Utrecht University, 3584CC Utrecht, The Netherlands*; orcid.org/0000-0002-4650-9473

Elleke J. van Harten – *Soft Condensed Matter, Utrecht University, 3584CC Utrecht, The Netherlands*

Complete contact information is available at: <https://pubs.acs.org/doi/10.1021/acs.jpcllett.0c01250>

Notes

The authors declare no competing financial interest.

■ ACKNOWLEDGMENTS

The authors thank A. van Blaaderen and B. M. Weckhuysen for helpful comments and suggestions. This work was supported by The Netherlands Center for Multiscale Catalytic Energy Conversion (MCEC), an NWO Gravitation Programme funded by the Ministry of Education, Culture and Science of the government of The Netherlands. F.T.R. acknowledges financial support from The Netherlands Organisation for Scientific Research NWO (VENI grant number 722.017.002).

■ REFERENCES

- (1) Alivisatos, A. P. Semiconductor Clusters, Nanocrystals, and Quantum Dots. *Science* **1996**, *271*, 933–937.
- (2) Kovalenko, M. V.; Manna, L.; Cabot, A.; Hens, Z.; Talapin, D. V.; Kagan, C. R.; Klimov, V. I.; Rogach, A. L.; Reiss, P.; Milliron, D. J.; Guyot-Sionnest, P.; Konstantatos, G.; Parak, W. J.; Hyeon, T.; Korgel, B. A.; Murray, C. B.; Heiss, W. Prospects of Nanoscience with Nanocrystals. *ACS Nano* **2015**, *9*, 1012–1057.
- (3) Sher, P. H.; Smith, J. M.; Dalgarno, P. A.; Warburton, R. J.; Chen, X.; Dobson, P. J.; Daniels, S. M.; Pickett, N. L.; O'Brien, P.

Power Law Carrier Dynamics in Semiconductor Nanocrystals at Nanosecond Timescales. *Appl. Phys. Lett.* **2008**, *92*, 101111.

(4) Jones, M.; Lo, S. S.; Scholes, G. D. Quantitative Modeling of the Role of Surface Traps in CdSe/CdS/ZnS Nanocrystal Photoluminescence Decay Dynamics. *Proc. Natl. Acad. Sci. U. S. A.* **2009**, *106*, 3011–3016.

(5) Pevere, F.; Sangghaleh, F.; Bruhn, B.; Sychugov, I.; Linnros, J. Rapid Trapping as the Origin of Nonradiative Recombination in Semiconductor Nanocrystals. *ACS Photonics* **2018**, *5*, 2990–2996.

(6) Guo, T.; Bose, R.; Zhou, X.; Gartstein, Y. N.; Yang, H.; Kwon, S.; Kim, M. J.; Lutfullin, M.; Sinatra, L.; Gereige, I.; Al-Saggaf, A.; Bakr, O. M.; Mohammed, O. F.; Malko, A. V. Delayed Photoluminescence and Modified Blinking Statistics in Alumina-Encapsulated Zero-Dimensional Inorganic Perovskite Nanocrystals. *J. Phys. Chem. Lett.* **2019**, *10*, 6780–6787.

(7) Montanarella, F.; Biondi, M.; Hinterding, S. O. M.; Vanmaekelbergh, D.; Rabouw, F. T. Reversible Charge-Carrier Trapping Slows Förster Energy Transfer in CdSe/CdS Quantum-Dot Solids. *Nano Lett.* **2018**, *18*, 5867–5874.

(8) Tachiya, M.; Seki, K. Unified Explanation of the Fluorescence Decay and Blinking Characteristics of Semiconductor Nanocrystals. *Appl. Phys. Lett.* **2009**, *94*, No. 081104.

(9) Whitham, P. J.; Knowles, K. E.; Reid, P. J.; Gamelin, D. R. Photoluminescence Blinking and Reversible Electron Trapping in Copper-Doped CdSe Nanocrystals. *Nano Lett.* **2015**, *15*, 4045–4051.

(10) Rabouw, F. T.; Kamp, M.; Van Dijk-Moes, R. J. A.; Gamelin, D. R.; Koenderink, A. F.; Meijerink, A.; Vanmaekelbergh, D. Delayed Exciton Emission and Its Relation to Blinking in CdSe Quantum Dots. *Nano Lett.* **2015**, *15*, 7718–7725.

(11) Whitham, P. J.; Marchioro, A.; Knowles, K. E.; Kilburn, T. B.; Reid, P. J.; Gamelin, D. R. Single-Particle Photoluminescence Spectra, Blinking, and Delayed Luminescence of Colloidal CuInS₂ Nanocrystals. *J. Phys. Chem. C* **2016**, *120*, 17136–17142.

(12) Rabouw, F. T.; Van der Bok, J. C.; Spinicelli, P.; Mahler, B.; Nasilowski, M.; Pedetti, S.; Dubertret, B.; Vanmaekelbergh, D. Temporary Charge Carrier Separation Dominates the Photoluminescence Decay Dynamics of Colloidal CdSe Nanoplatelets. *Nano Lett.* **2016**, *16*, 2047–2053.

(13) Marchioro, A.; Whitham, P. J.; Knowles, K. E.; Kilburn, T. B.; Reid, P. J.; Gamelin, D. R. Tunneling in the Delayed Luminescence of Colloidal CdSe, Cu⁺-Doped CdSe, and CuInS₂ Semiconductor Nanocrystals and Relationship to Blinking. *J. Phys. Chem. C* **2016**, *120*, 27040–27049.

(14) Chirvony, V. S.; González-Carrero, S.; Suárez, I.; Galian, R. E.; Sessolo, M.; Bolink, H. J.; Martínez-Pastor, J. P.; Pérez-Prieto, J. Delayed Luminescence in Lead Halide Perovskite Nanocrystals. *J. Phys. Chem. C* **2017**, *121*, 13381–13390.

(15) Marchioro, A.; Whitham, P. J.; Nelson, H. D.; De Siena, M. C.; Knowles, K. E.; Polinger, V. Z.; Reid, P. J.; Gamelin, D. R. Strong Dependence of Quantum-Dot Delayed Luminescence on Excitation Pulse Width. *J. Phys. Chem. Lett.* **2017**, *8*, 3997–4003.

(16) Klimov, V. I.; Mikhailovsky, A. A.; Xu, S.; Malko, A.; Hollingsworth, J. A.; Leatherdale, C. A.; Eisler, H. J.; Bawendi, M. G. Optical Gain and Stimulated Emission in Nanocrystal Quantum Dots. *Science* **2000**, *290*, 314–317.

(17) Schwartz, O.; Tenne, R.; Levitt, J. M.; Deutsch, Z.; Itzhakov, S.; Oron, D. Colloidal Quantum Dots as Saturable Fluorophores. *ACS Nano* **2012**, *6*, 8778–8782.

(18) Kuno, M.; Fromm, D. P.; Hamann, H. F.; Gallagher, A.; Nesbitt, D. J. “On”/“off” Fluorescence Intermittency of Single Semiconductor Quantum Dots. *J. Chem. Phys.* **2001**, *115*, 1028–1040.

(19) Kuno, M.; Fromm, D. P.; Hamann, H. F.; Gallagher, A.; Nesbitt, D. J. Nonexponential “Blinking” Kinetics of Single CdSe Quantum Dots: A Universal Power Law Behavior. *J. Chem. Phys.* **2000**, *112*, 3117–3120.

(20) Polland, H.-J.; Schultheis, L.; Kuhl, J.; Göbel, E. O.; Tu, C. W. Lifetime Enhancement of Two-Dimensional Excitons by the Quantum-Confined Stark Effect. *Phys. Rev. Lett.* **1985**, *55*, 2610–2613.

(21) Wen, G. W.; Lin, J. Y.; Jiang, H. X.; Chen, Z. Quantum-Confined Stark Effects in Semiconductor Quantum Dots. *Phys. Rev. B: Condens. Matter Mater. Phys.* **1995**, *52*, 5913–5922.

(22) Müller, J.; Lupton, J. M.; Rogach, A. L.; Feldmann, J.; Talapin, D. V.; Weller, H. Monitoring Surface Charge Migration in the Spectral Dynamics of Single CdSe CdS Nanodot/Nanorod Heterostructures. *Phys. Rev. B: Condens. Matter Mater. Phys.* **2005**, *72*, 205339.

(23) Kraus, R. M.; Lagoudakis, P. G.; Rogach, A. L.; Talapin, D. V.; Weller, H.; Lupton, J. M.; Feldmann, J. Room-Temperature Exciton Storage in Elongated Semiconductor Nanocrystals. *Phys. Rev. Lett.* **2007**, *98*, No. 017401.

(24) Zhang, L.; Lv, B.; Yang, H.; Xu, R.; Wang, X.; Xiao, M.; Cui, Y.; Zhang, J. Quantum-Confined Stark Effect in the Ensemble of Phase-Pure CdSe/CdS Quantum Dots. *Nanoscale* **2019**, *11*, 12619–12625.

(25) Empedocles, S. A.; Bawendi, M. G. Quantum-Confined Stark Effect in Single CdSe Nanocrystallite Quantum Dots. *Science* **1997**, *278*, 2114–2117.

(26) Zang, H.; Cristea, M.; Shen, X.; Liu, M.; Camino, F.; Cotlet, M. Charge Trapping and De-Trapping in Isolated CdSe/ZnS Nanocrystals under an External Electric Field: Indirect Evidence for a Permanent Dipole Moment. *Nanoscale* **2015**, *7*, 14897–14905.

(27) Rothenberg, E.; Kazes, M.; Shaviv, E.; Banin, U. Electric Field Induced Switching of the Fluorescence of Single Semiconductor Quantum Rods. *Nano Lett.* **2005**, *5*, 1581–1586.

(28) Park, K.; Deutsch, Z.; Li, J. J.; Oron, D.; Weiss, S. Single Molecule Quantum-Confined Stark Effect Measurements of Semiconductor Nanoparticles at Room Temperature. *ACS Nano* **2012**, *6*, 10013–10023.

(29) Fernée, M. J.; Plakhotnik, T.; Louyer, Y.; Littleton, B. N.; Potzner, C.; Tamarat, P.; Mulvaney, P.; Lounis, B. Spontaneous Spectral Diffusion in CdSe Quantum Dots. *J. Phys. Chem. Lett.* **2012**, *3*, 1716–1720.

(30) Fernée, M. J.; Littleton, B.; Plakhotnik, T.; Rubinsztein-Dunlop, H.; Gómez, D. E.; Mulvaney, P. Charge Hopping Revealed by Jitter Correlations in the Photoluminescence Spectra of Single CdSe Nanocrystals. *Phys. Rev. B: Condens. Matter Mater. Phys.* **2010**, *81*, 155307.

(31) Chen, O.; Zhao, J.; Chauhan, V. P.; Cui, J.; Wong, C.; Harris, D. K.; Wei, H.; Han, H. S.; Fukumura, D.; Jain, R. K.; Bawendi, M. G. Compact High-Quality CdSe-CdS Core-Shell Nanocrystals with Narrow Emission Linewidths and Suppressed Blinking. *Nat. Mater.* **2013**, *12*, 445–451.

(32) Brokmann, X.; Coolen, L.; Dahan, M.; Hermier, J. P. Measurement of the Radiative and Nonradiative Decay Rates of Single CdSe Nanocrystals through a Controlled Modification of Their Spontaneous Emission. *Phys. Rev. Lett.* **2004**, *93*, 107403.

(33) Galland, C.; Ghosh, Y.; Steinbrück, A.; Hollingsworth, J. A.; Htoon, H.; Klimov, V. I. Lifetime Blinking in Nonblinking Nanocrystal Quantum Dots. *Nat. Commun.* **2012**, *3*, 908.

(34) Efros, A. L.; Nesbitt, D. J. Origin and Control of Blinking in Quantum Dots. *Nat. Nanotechnol.* **2016**, *11*, 661–671.

(35) Kalyuzhny, G.; Murray, R. W. Ligand Effects on Optical Properties of CdSe Nanocrystals. *J. Phys. Chem. B* **2005**, *109*, 7012–7021.

(36) Jones, M.; Kumar, S.; Lo, S. S.; Scholes, G. D. Exciton Trapping and Recombination in Type II CdSe/CdTe Nanorod Heterostructures. *J. Phys. Chem. C* **2008**, *112*, 5423–5431.

(37) Mooney, J.; Krause, M. M.; Saari, J. I.; Kambhampati, P. Challenge to the Deep-Trap Model of the Surface in Semiconductor Nanocrystals. *Phys. Rev. B: Condens. Matter Mater. Phys.* **2013**, *87*, 081201R.

(38) Liu, S.; Borys, N. J.; Sapra, S.; Eychmüller, A.; Lupton, J. M. Localization and Dynamics of Long-Lived Excitations in Colloidal Semiconductor Nanocrystals with Dual Quantum Confinement. *ChemPhysChem* **2015**, *16*, 1663–1669.

(39) Van Driel, A. F.; Allan, G.; Delerue, C.; Lodahl, P.; Vos, W. L.; Vanmaekelbergh, D. Frequency-Dependent Spontaneous Emission

Rate from CdSe and CdTe Nanocrystals: Influence of Dark States. *Phys. Rev. Lett.* **2005**, *95*, 236804.

(40) Sallen, G.; Tribu, A.; Aichele, T.; André, R.; Besombes, L.; Bougerol, C.; Richard, M.; Tatarenko, S.; Kheng, K.; Poizat, J. P. Subnanosecond Spectral Diffusion Measurement Using Photon Correlation. *Nat. Photonics* **2010**, *4*, 696–699.

(41) Ihara, T.; Kanemitsu, Y. Spectral Diffusion of Neutral and Charged Exciton Transitions in Single CdSe/ZnS Nanocrystals Due to Quantum-Confined Stark Effect. *Phys. Rev. B: Condens. Matter Mater. Phys.* **2014**, *90*, 195302.

(42) Ihara, T.; Kanemitsu, Y. Absorption Cross-Section Spectrum of Single CdSe/ZnS Nanocrystals Revealed through Photoluminescence Excitation Spectroscopy. *Phys. Rev. B: Condens. Matter Mater. Phys.* **2015**, *92*, 155311.

(43) Fernée, M. J.; Littleton, B. N.; Rubinsztein-Dunlop, H. Detection of Bright Trion States Using the Fine Structure Emission of Single CdSe/ZnS Colloidal Quantum Dots. *ACS Nano* **2009**, *3*, 3762–3768.

(44) Empedocles, S. A.; Norris, D. J.; Bawendi, M. G. Photoluminescence Spectroscopy of Single CdSe Nanocrystallite Quantum Dots. *Phys. Rev. Lett.* **1996**, *77*, 3873–3876.

(45) Park, Y. S.; Lim, J.; Klimov, V. I. Asymmetrically Strained Quantum Dots with Non-Fluctuating Single-Dot Emission Spectra and Subthermal Room-Temperature Linewidths. *Nat. Mater.* **2019**, *18*, 249–255.